TRANSIENT MODEL FOR THE START-UP OF A THIXOTROPIC FLUID FLOW

Leandro Lourenço Vieira da Rocha, leandrolvrocha@gmail.com
Gabriel Merhy de Oliveira, gabrielmerhy@hotmail.com
Cezar Otaviano Ribeiro Negrão, negrao@utfpr.edu.br
Admilson T. Franco, admilson@utfpr.edu.br
UTFPR - Federal University of Technology - Paraná – Av. Sete de Setembro, 3165, CEP 80.230-901 – Curitiba-PR-Brazil

Andre Leibsohn Martins, aleibsohn@petrobras.com.br
Roni Abensur Gandelman, roniag@petrobras.com.br
TEP/CENPES - PETROBRAS S/A – Cidade Universitária, Q.7, Ilha do Fundão, CEP 21.941-915, Rio de Janeiro-RJ

Abstract. *The present work describes a mathematical model for the restart of a gelled fluid in pipelines. This axial, compressible and transient flow of a thixotropic fluid requires pressures higher than the usual operation ones in order to break up the gel. The model is based on the mass and momentum conservation equations and on a state equation for the calculation of the fluid density as a function of the pressure. Furthermore, a thixotropic model is used to describe the time-dependent behavior of the rheological properties. The governing equations are discretized by the Finite Volume Method using the fully implicit formulation and the first-order upwind scheme. The resulting non-linear algebraic equations are iteratively solved. The results of a non-Newtonian Bingham fluid flow presented good agreement with the literature. In addition, a sensibility analysis to the flow dimensionless parameters was carried out. The model can be applied to predict the time-dependent pressure field in waxy crude oil production lines and to measure the pressure peaks during the restart of drilling fluid operations.*

Keywords*: Start-up flow, drilling fluid, thixotropic model, compressible flow, transient flow.*

1. INTRODUCTION

Fluids that gelify when not submitted to shear stress are largely employed by several industries. An example is the oil industry, which uses a wide variety of those materials, such as drilling fluids and waxy crude oils.

The drilling fluid is designed to build up a gel-like structure, when at rest, in order to avoid cuttings to drop at the bore bottom and therefore to prevent the bit obstruction. As consequence, high pressures, which can be larger than the formation pressure and can damage the well, are needed to break the gel.

On the other hand, waxy crude oils can be produced at relatively low temperatures, below its pour point. When production is stopped for maintenance reason the oil can gelify, and high pump pressures are also necessary to break gel up. These pressures can even overcome the usual operation pressure.

The mathematical model of the fluid flow is quite important to understand the phenomenon and prediction of the pressure peaks during the circulation start-up. Some works are found in the literature, but most of them are dedicated to the start-up of waxy crude oils at low temperatures. The Sestak's *et al*. (1987), Cawkwell's *et al*. (1987), Chang's *et al*. (1999) and Davidson's *et al*. (2004) works consider that initially a gelified material fills a pipe and then it is displaced by a non-gelified fluid. Chang *et al*. (1999) and Sestak *et al*. (1987) disregard the transient term on the momentum conservation equation and consider equilibrium of pressure and viscous forces all the time. The transient changes are only due to the time variation of rheological properties. Davidson *et al*. (2004) has improved Chang's *et al*. (1999) model by including the compressibility effect of the gelified material, but yet did not take into account the transient term in the momentum conservation equation. Despite the fact the inertia terms in the momentum conservation equation were disregarded, Cawkwell *et al*. (1987), on the other hand, dealt the flow as transient and compressible. Their numerical results, however, seems inaccurate, as the employed computational grids are course. Vinay *et al*. (2006) presented a two-dimensional, transient model to simulate the start-up of compressible flows of a Bingham fluid. After that, Vinay *et al*. (2007) discussed a one-dimensional model and compare their results to the 2D model results, showing good agreement. However, Vinay *et al*. (2007) said the 1D model is more efficient, as the computational time is reduced from days and hours to minutes or even seconds. In a newer work, Wachs *et al*. (2008), in order to reduce the computational time and to have better agreement with 2D model, developed one model characterized like 1.5D, where they mix the 1D with 2D model. In this work, the authors also evaluate the compressibility and thixotropic characteristics of the fluid in the start-up flow.

Some of the revised articles (Cawkwell *et al*., 1987; Chang *et al*., 1999; Davidson *et a*l., 2004; Wachs *et al*., 2008) had considered the thixotropy by including a time-dependent equation for the rheological properties.

The current work presents a one-dimensional transient compressible mathematical model for the start-up of gelified fluids in pipes. Differently from some above works, both transient and inertia terms are considered. Besides, the concept of friction factor is employed to account for viscous effect, which simplifies the implementation of different constitutive

equations in the momentum conservation equation. The conservation equations of mass and momentum are discretized by using the implicit finite volume method and the first order upwind approach. The discretized equations, together with an equation of state and a constitutive equation (a simple thixotropic model), are solved iteratively.

2. MATHEMATICAL MODEL

2.1. Problem geometry and hypotheses

The considered geometry is a concentric annular pipe of length L, inclined at a β angle with the horizontal. The pipe internal diameter is D_1 and external one, D_2, as shown in Fig. 1. The domain is reduced to a circular pipe as its internal diameter becomes null.

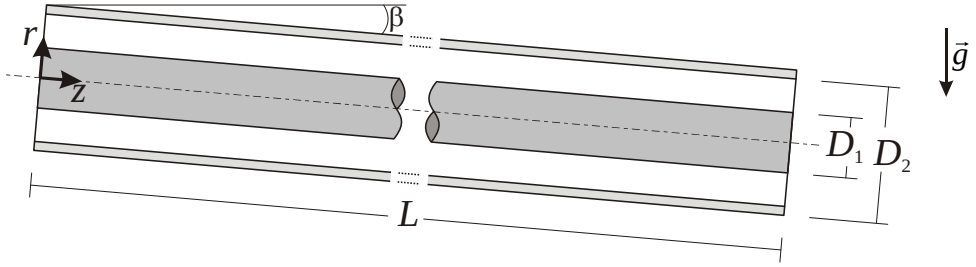

Figure 1. Annular pipe geometry

The flow is assumed compressible, isothermal and one-dimensional. Initially, the fluid rests within the pipe and suddenly the pipe inlet is submitted to a pressure step-change. The fluid within the pipe is thus continuously replaced by the fluid being injected. The injected fluid is considered to enter the pipe with the same properties of the outlet fluid.

The pipe is admitted completely rigid and therefore, does not undergo any kind of strain. The shear stress on the pipe walls is evaluated by employing the friction factor for both Newtonian and Non-Newtonian Bingham fluids.

2.2. Governing equations

As the fluid flow is considered one-dimensional (Fig. 1), the conservation equations of mass and momentum can be written, respectively, as:

$$\frac{\partial \rho}{\partial t} + \frac{\partial (\rho V)}{\partial z} = 0 \tag{1}$$

$$\frac{\partial (\rho V)}{\partial t} + \frac{\partial (\rho V V)}{\partial z} = -\frac{\partial P}{\partial z} - \pi \left(D_1 \tau_1 + D_2 \tau_2 \right) + \rho g \sin \beta \tag{2}$$

where ρ, V and P are average values of density, velocity and pressure on the pipe cross sectional area, respectively. t is the time and z is the axial position. g is the gravity and β is the angle with the horizontal. The second term on the right hand side of Eq. (2) is the shear forces per unit of length on the annular walls which affect the average flow. These forces can be represented by the concept of friction factor:

$$\pi \left(D_1 \tau_1 + D_2 \tau_2 \right) = \frac{2 f \rho V^2}{D_h} \tag{3}$$

where f is the Fanning friction factor that depends on the fluid properties and flow geometry (circular or annular pipe). D_h is the hydraulic diameter, which is $D_2 - D_1$ for the annular and D_2, for the circular pipe.

To consider the fluid compressibility effects, is used the concept of isothermal compressibility, which is defined as (Anderson, 1990):

$$\alpha = \frac{1}{\rho} \frac{\partial \rho}{\partial P}\bigg|_T \tag{4}$$

As the flow is considered isotherm, the density is only dependent on pressure and if the compressibility is admitted constant within a range of pressure, Eq. (4) can be integrated from a reference state to any other state, resulting on an equation for pressure calculation:

$$P = P_o + \frac{1}{\alpha}\ln\left(\frac{\rho}{\rho_o}\right) \tag{5}$$

where ρ_o and P_o are, respectively, density and pressure at the reference state. The compressibility can yet be related to the wave speed, a, by the following equation (Anderson, 1990):

$$\alpha = \frac{1}{\rho_o a^2} \tag{6}$$

The constitutive equations are implicitly taken into account in the calculation of the friction factor coefficient. In order to consider the thixotropic effects, Chang *et al.* (1999) proposed a time-dependent Bingham equation:

$$\tau(t) = \tau_y(t) + \eta\dot{\gamma} \tag{7}$$

where $\tau_y(t)$ is a Bingham yield stress which is time-dependent:

$$\tau_y(t) = \frac{\tau_y(0) - \tau_y(\infty)}{1 + \kappa\, t} + \tau_y(\infty) \tag{8}$$

$\tau_y(0)$ and $\tau_y(\infty)$ are apparent yield stress at time $t = 0$ and $t = \infty$, respectively, and κ is a constant that characterizes the gel consistency.

2.3. Dimensionless governing equations

The pipe length, the time for the pressure wave to travel the length of the pipe and the reference density are defined as scales for the dimensionless axial position, time and density, respectively:

$$\bar{z} = \frac{z}{L},\quad \bar{t} = t\frac{a}{L} \text{ and } \quad \bar{\rho} = \frac{\rho}{\rho_o} \tag{9}$$

The dimensionless pressure and velocity are based on reference values. For one prescribed inlet pressure (P_P), the reference velocity (V_P) is calculated based on the steady-state velocity of a Newtonian fluid:

$$V_P = \frac{P_P D_h^2}{32\eta L}\frac{1}{\zeta} \tag{10}$$

where η is the fluid viscosity and the geometric parameter for the annular space is defined as:

$$\zeta = \frac{\left(D_2 - D_1\right)^2}{D_2^2 + D_1^2 - \dfrac{\left(D_2^2 - D_1^2\right)}{\ln\left(D_2/D_1\right)}} \tag{11}$$

Therefore, the dimensionless values of pressure and velocity are defined, respectively as:

$$\bar{P}\left(\bar{z},\bar{t}\right) = \frac{P\left(z,t\right) - P\left(z,t=0\right)}{P_P} \tag{12}$$

$$\bar{V}\left(\bar{z},\bar{t}\right) = \frac{V\left(z,t\right)}{V_P} \tag{13}$$

Substituting the dimensionless variables in the governing equations (1), (2) and (4), the following equations are found:

$$\left(\frac{32\zeta}{\mathrm{Re}\,\delta\alpha^*}\right)^{1/2}\frac{\partial\bar{\rho}}{\partial\bar{t}} + \frac{\partial(\bar{\rho}\bar{V})}{\partial\bar{z}} = 0 \tag{14}$$

$$\left(\frac{32\zeta}{\mathrm{Re}\,\delta\alpha^*}\right)^{1/2}\frac{\partial(\bar{\rho}\bar{V})}{\partial\bar{t}} + \frac{\partial(\bar{\rho}\bar{V}\bar{V})}{\partial\bar{z}} = -\frac{32\zeta}{\mathrm{Re}\,\delta}\frac{\partial\bar{P}}{\partial\bar{z}} - 2f\bar{\rho}\bar{V}^2 + \frac{32\zeta}{\mathrm{Re}\,\delta}\frac{g^*}{\alpha^*}\bar{\rho} \tag{15}$$

$$\frac{d\overline{\rho}}{d\overline{P}} = \alpha^* \overline{\rho} \tag{16}$$

where Re, α^*, g^* and δ are, respectively, the Reynolds number, the dimensionless compressibility, the dimensionless gravity and the aspect ratio, which are defined as:

$$\mathrm{Re} = \frac{\rho_o V_P D_h}{\eta}, \quad \alpha^* = \alpha P_P, \quad \mathrm{g}^* = \frac{gL\sin\beta}{a^2} \quad \text{and} \quad \delta = \frac{D_h}{L} \tag{17}$$

Besides, the Bingham number is defined as:

$$\mathrm{B} = 4\frac{\tau_y}{P_P}\frac{L}{D_h} \tag{18}$$

According to this definition, the flow will only take place if $\mathrm{B} < 1.0$. In case, $\mathrm{B} \geq 1.0$, the gel is not completely broken and the flow does not occur. A non-zero pressure gradient is established along the whole pipe for $\mathrm{B} \leq 1.0$, and in part of the pipe, for $\mathrm{B} > 1.0$. In a non-started flow case, the length of the non-zero pressure gradient region is inversely proportional to the Bingham number, such as: $\overline{z} = 1/\mathrm{B}$. For a thixotropic material, which τ_y is time-dependent, the Bingham number changes with time and it can be initially larger than one. As time elapses, τ_y reduces and the Bingham number becomes smaller than one and therefore the flow is fully established. In Section 4, these cases will be further discussed.

2.4. Initial and boundary conditions

The fluid is considered to rest within the pipe and, therefore, the initial velocity field is zero ($\overline{V}(\overline{z}, \overline{t} = 0) = 0$). As the pipe is inclined with the horizontal, the density varies with the fluid weight and consequently, with the position:

$$\overline{\rho}\left(\overline{z}, \overline{t} = 0\right) = \left(1 - g^* \overline{z}\right)^{-1} \tag{19}$$

By substituting the density field (Eq. (19)) in Eq. (16) and integrating it, the initial pressure field can be obtained:

$$\overline{P}(\overline{z}, \overline{t} = 0) = -\frac{1}{\alpha^*}\ln\left(1 - g^* \overline{z}\right) \tag{20}$$

In case the pipe is placed horizontally, $g^* = 0$, Eq. (19) is reduced to $\overline{\rho}\left(\overline{z}, \overline{t} = 0\right) = 1$ and the dimensionless initial pressure field is null $\overline{P}(\overline{z}, \overline{t} = 0) = 0$.

The start-up takes place when a pump delivers fluid to the pipe and the gelified fluid begins to be gradually displaced. To represent that, one type of boundary conditions can be established at the pipe inlet: constant pressure. In this case, inlet dimensionless pressure can be represented by a unit step function ($\overline{P}(\overline{z} = 0, \overline{t}) = \mathrm{us}\left(\overline{t}\right)$). At the pipe outlet, is adopted that the density and the pressure are kept constants with the initial values.

2.5. Friction Factor

The friction factor depends on fluid properties, flow type and geometry. In the current work, the flow is considered laminar. For a laminar flow of a Non-Newtonian Bingham fluid in a circular pipe ($\zeta = 1$), the Fanning friction factor is written as a function of the Reynolds ($\mathrm{Re}_{z,t}$) and Hedstrom ($\mathrm{He}_{z,t} = \rho\tau_y D_h^{\,2} / \eta^2$) numbers (Chang *et al.*,1999):

$$f_P = \frac{16}{\mathrm{Re}_{z,t}}\left(1 + \frac{\mathrm{He}_{z,t}}{6\,\mathrm{Re}_{z,t}} - \frac{\mathrm{He}_{z,t}^4}{3f^3\,\mathrm{Re}_{z,t}^7}\right) \tag{21}$$

where the subscript P means the circular pipe. The subscripts t and z indicate the Reynolds and Hedstrom numbers are dependent on the time and the axial position. Eq. (21) is simplified to the friction factor of laminar Newtonian flows as the Hedstrom number, or yield stress, approaches zero.

For an annular pipe, Fontenot and Clark (1974) adapted the friction factor according to the following:

$$f_A = \frac{16}{\mathrm{Re}_{z,t}}\frac{\zeta}{\gamma} \tag{22}$$

where the index A means the annular space and γ is nominated conductance of the Bingham fluid which can be obtained by:

$$\gamma = 1 - \frac{\gamma \mathrm{He}_{z,t}}{8\,\mathrm{Re}_{z,t}} + \frac{1}{2}\left(\frac{\gamma \mathrm{He}_{z,t}}{12\,\mathrm{Re}_{z,t}}\right)^3 \tag{23}$$

For a zero yield stress, $\gamma = 1$, Eq. (22) becomes the correlation for the friction factor of the laminar annular flow. According to Fontenot and Clark (1974), flow with the product of conductance and Reynolds number smaller than 2000 ($\gamma\,\mathrm{Re}_{z,t} = 2000$) are considered laminar.

At the start-up, the velocity along the pipe is either zero or very close to it, and therefore, Eqs. (21) and (22) become indeterminate. For the Newtonian fluid flow, this indetermination can be easily eliminated by substituting the friction factor in Eq.(3), and the friction force term becomes a function of the average velocity. For the Bingham fluid flow in a circular pipe, Eq. (21) can be rearranged in order to obtain an expression for the product $f\,\mathrm{Re}_{z,t}^2$. As the Reynolds number tends to zero, the product $f\,\mathrm{Re}_{z,t}^2$ approaches $2\mathrm{He}_{z,t}$ and the indetermination can be removed. In an annular pipe, on the other hand, $f\,\mathrm{Re}_{z,t}^2$ tends to $\frac{4\zeta}{3}\mathrm{He}_{z,t}$ as $\mathrm{Re}_{z,t} \to 0$.

3. SOLUTION METHODOLOGY

The governing equations of the problem are discretized by the finite volume method, as proposed by Patankar (1980), by employing a staggered grid. The scalar variables are placed on the boundaries and the velocity in the center of the finite volumes. Figure 2 shows the grid scheme for an annular pipe. The domain is divided in N uniform finite volumes of length $\Delta\bar{z}$. Note in Fig. 2 that the $\bar{\rho}$ and $\bar{P}$ positions are denoted by the index i, and the $\bar{V}$ position by I. For this grid, i varies from 1 to $N+1$ and I, from 1 to N. The variables correspond to an average value across the pipe sectional area. The discretization of the equations is conducted by employing implicit formulation and the first order upwind scheme.

To solve the equations, initially, velocity and pressure are estimated for all finite volumes and the governing equations are solved sequentially, through the implementation in FORTRAN language, until convergence is reached.

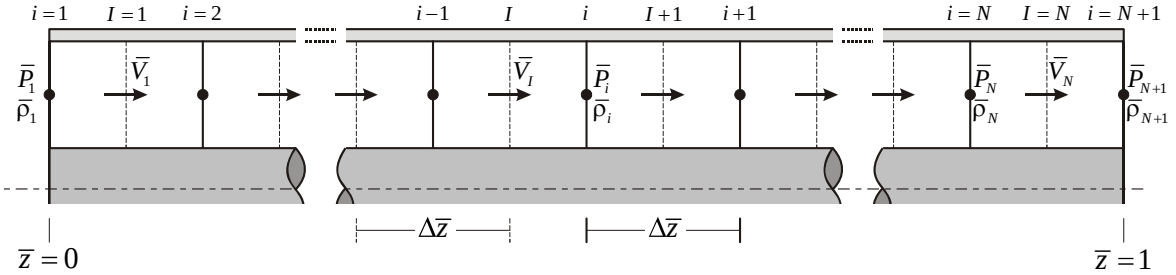

Figure 2. Grid scheme for the discretization of the equations

After this convergence, one advances one time step, repeating the calculations to obtain the fields of velocity and pressure. This process occurs repeatedly until the steady-state be reached.

The compressible transient problem is a hyperbolic one (Ferziger and Peric, 1996) and therefore, the time and space grids ($\Delta\bar{t}$ and $\Delta\bar{z}$) must be correlated in order to avoid numerical errors. These errors can cause instabilities, compromising the convergence or causing numerical diffusion or dispersion. Thus, to ensure the stability of the method, a condition of numerical stability proposed by Fortuna (2000) is used in this work.

4 RESULTS

4.1. Comparison with the literature

In order to validate the model for a non-Newtonian Bingham flow, some comparisons with Vinay's *et al.* (2007) results were conducted. They studied the Bingham fluid flow in a horizontal pipe with a constant pressure boundary condition. The parameters of this comparison are: $\mathrm{Re} = 0.25$, $\mathrm{B} = 0.2$, $\alpha^* = 1.0$, $\mathrm{g}^* = 0.0$, $\delta = 0.002$ e $\zeta = 1.0$.

Figure 3 compares the pressure field at several times. The time values showed in Fig. 3 are the ones used by Vinay *et al.* (2007), which have employed different time normalization. According to Vinay *et al.* (2007), the $\bar{t} = 63.26$ curve

is the steady-state pressure field. Note the results are very similar and that the average percent difference is 3.6%. The results of Vinay *et al*. (2007) were extracted by employing a computer program.

Figure 4 presents the inlet and outlet velocity variations with time, for both models. The average percent difference between the inlet velocity results is 2.6% and the outlet velocity ones 2.1%. Although Vinay *et al*. (2007) claimed the problem had reached, the steady-state at $\overline{t} = 63.26$, one can see the inlet and the outlet velocity are still varying considerably at this time.

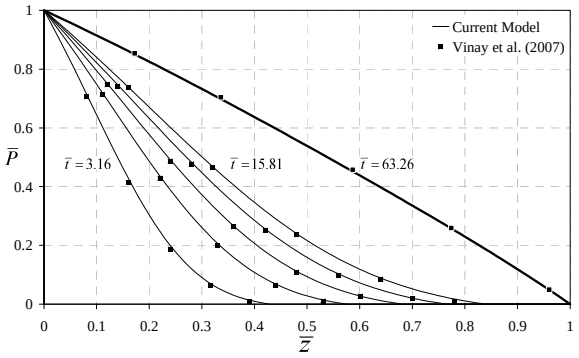

Figure 3. Pressure fields at the discrete times $\overline{t} = 3.16$, 6.32, 9.49, 12.65, 15.81 and $\overline{t} = 63.26$ (bold line). Comparison with Vinay *et al*. (2007)

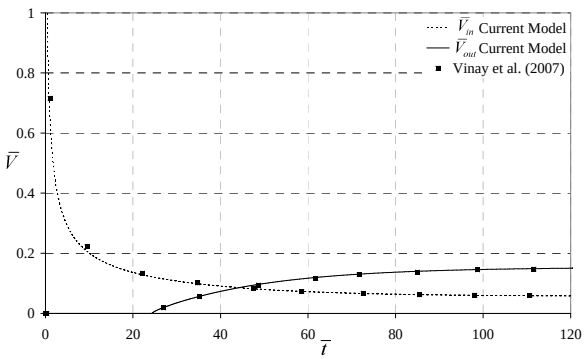

Figure 4. Temporal inlet (continuous line) and outlet velocity (discontinuous line) variations. Comparison with Vinay *et al*. (2007)

4.2. Sensitivity analysis

In this section, the influence of each dimensionless parameter defined in Section 2.3 is analyzed. Initially, the effect of the aspect ratio is examined. Next, the influence of g^*/α^* for low and high compressibility flows is checked. Then, the effect of the Reynolds number for different dimensionless compressibility is investigated. Finally, the dependency of the fluid flow on the Bingham number is evaluated.

4.2.1. The effect of aspect ratio

Figure 5 presents the pressure change with time at the position $\overline{z} = 0.5$ for different aspect ratio, $\mathrm{Re} = 100$, $\mathrm{B} = 0.5$, $\alpha^* = 0.01$, $g^* = 0.1$ and $\zeta = 1.0$. For small aspect ratio ($\delta = 0.00001$), the pipe is long enough to dissipate the pressure wave and reflections are not seen. The higher the aspect ratio, the smaller the dissipation and consequently, the higher the pressure peaks. For shorter pipes ($\delta = 0.001$ and $\delta = 0.01$), the energy of the pressure wave is high enough to reflect repeatedly with the frequency; the frequency depends only on the wave speed. Nevertheless, the higher the aspect ratio the higher pressure peak magnitude. The first pressure peaks are 0.5%, 31% and 53% higher than their steady-state values, for $\delta = 0.0001$, 0.001 and 0.01, respectively. As observed for the Reynolds number, the steady state pressure [$\overline{P}_{SS}\left(\overline{z} = 0.5\right) = 0.5013$] is aspect ratio independent.

Therefore, when the pipe length is long enough, there is a large extension to pressure wave dissipation, and the pressure propagates smoothly. On the other hand, for short pipes, the length is not long enough for pressure dissipation and significant pressure changes take place.

4.2.2. The effect of dimensionless gravity

For a vertical pipe, the fluid density varies with the depth because of its own weight and compressibility. The dimensionless pressures computed for a horizontal ($g^* = 0.0$) and a vertical pipe ($g^* = 0.1$) are compared in Fig. 6. The pressure wave dissipation is larger in horizontal than in vertical position and consequently, the pressure peaks are higher in the later. Additionally, for the less compressible case ($\alpha^* = 0.001$), the pressure peaks computed for the vertical pipe are delayed in comparison to the horizontal case. This is due to the density increase and consequently, the wave speed reduction. The pressure peak delay shown in Fig. 6 is $\Delta\overline{t} = 0.03$, and peak magnitude is 6.1% higher than the horizontal pipe value. Although the pressure peak delay increases with time (e.g. the third peak is 0.14 delayed), the pressure peak difference reduces with it. The third peak is only 3.0% higher than its horizontal counterpart. For higher compressible flow, note that pressure peaks do not take place. It occurs due to the pressure wave dissipation in this case be greater than in a less compressible flow. However, it can be visualized in Fig. 6 that the effect of the dimensionless gravity is the same that observed for less compressible flow.

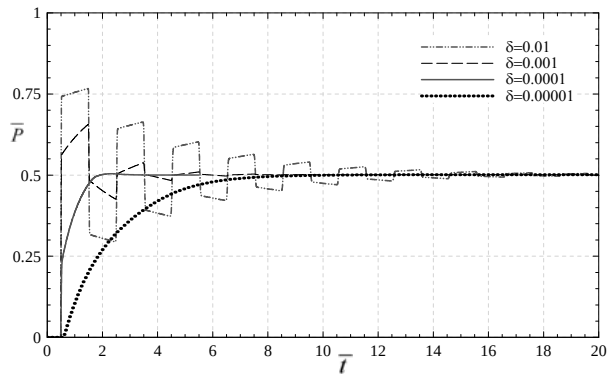

Figure 5. The effect of the aspect ratio on the temporal pressure change at $\overline{z} = 0.5$. $\mathrm{Re} = 100.0$ $B = 0.5$, $\alpha^* = 0.01$, $g^* = 0.1$, $\delta = 0.0001$ and $\zeta = 1.0$

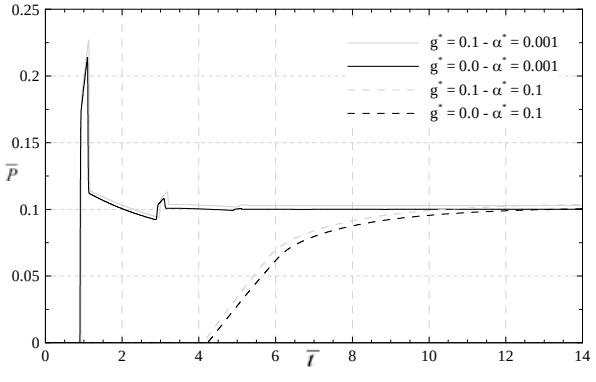

Figure 6. The effect of $g*/\alpha*$ on the temporal pressure change at $\overline{z} = 0.9$. $\mathrm{Re} = 100.0$, $B = 0.5$, $\delta = 0.0001$ and $\zeta = 1.5$

4.2.3. The effect of the Reynolds number

The influence of the Reynolds number on the pressure change with time at the middle of the pipe ($\overline{z} = 0.5$) can be observed in Fig. 7. In this analysis, the Bingham number, the compressibility, the dimensionless gravity, the aspect ratio and ζ are kept constant at the values $\mathrm{B} = 0.5$, $\alpha^* = 0.01$, $g^* = 0.1$, $\delta = 0.0001$ e $\zeta = 1.5$. As the inertia effect reduces in comparison to the viscous (reduction of Reynolds number), the dissipation of the pressure wave increases, causing a delay in the flow start-up. Nevertheless, the start-up times for $\mathrm{Re} = 100$ and $\mathrm{Re} = 1000$ are almost the same. On the other hand, the dissipation effect also affects the necessary time for the steady-state to be reached: the smaller the Reynolds number, the slower the pressure change. However, the increase of the Reynolds number makes the pressure unstable as the pressure reflects several times before its complete dissipation. This instability increases the time for the pressure to achieve the steady-state. Although the steady-state is not shown in Fig. 7 for $\mathrm{Re} = 1$, the steady-state pressure [$\overline{P}_{SS}\left(\overline{z} = 0.5\right) = 0.5005$] is the same for all Reynolds numbers.

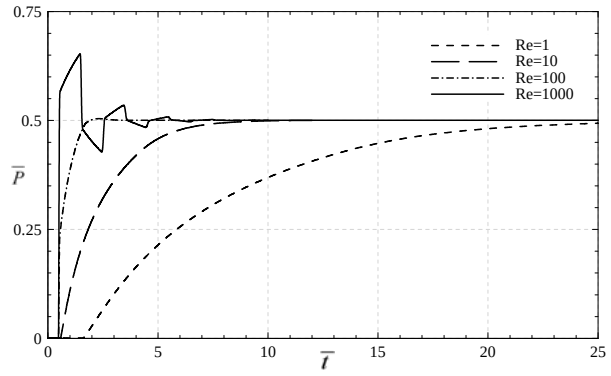

Figure 7. The effect of the Reynolds number on the temporal pressure change at $\overline{z} = 0.5$. $B = 0.5$, $\alpha^* = 0.01$, $g^* = 0.1$, $\delta = 0.0001$ and $\zeta = 1.5$.

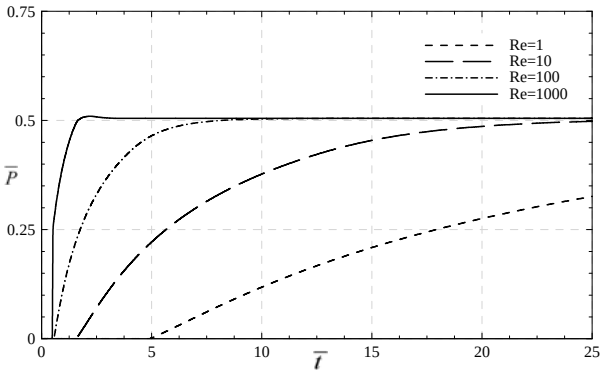

Figure 8. The effect of the Reynolds number on the temporal pressure change at $\overline{z} = 0.5$. $B = 0.5$, $\alpha^* = 0.1$, $g^* = 0.1$, $\delta = 0.0001$ and $\zeta = 1.5$.

The effect of the Reynolds number was also evaluated for higher compressible flow ($\alpha^* = 0.1$). Figure 8 shows the pressure change at the middle of the pipe. In comparison to the low compressibility flow, the steady-state pressure has increased slightly to 0.5047, but it is still Reynolds number independent. Nevertheless, the start-up delay is more evident and pressure reflections do not occur, even at high Reynolds number, as higher compressibility favors pressure dissipation. Only a slight peak is observed at $\mathrm{Re} = 1000$, which is due to the first pressure wave movement.

4.2.4. The effect of Bingham number

As mentioned earlier, the magnitude of the inlet pressure defines if the fluid flow of a Bingham fluid occurs or not. The relation of the inlet pressure and the yield stress is established by the Bingham number. When this parameter is smaller than the unity, the fluid flow takes place and the steady-state velocity is non-zero. For $\mathrm{B} \geq 1.0$, the flow initializes near the pipe inlet, but soon after the fluid velocity drops to zero. Figure 9 to 12 show some results for

different Bingham numbers: two for $B<1.0$, one for $B=1.0$ and a fourth one for a time varying Bingham number (thixotropic fluid).

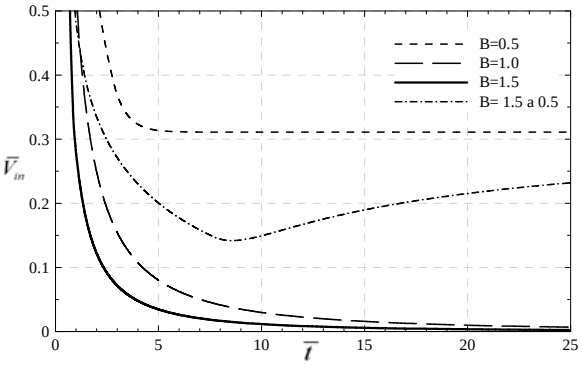

Figure 9. The effect of the Bingham number on the temporal inlet velocity variation. $Re=100.0$, $\alpha^*=0.01$, $g^*=0.1$, $\delta=0.0001$ and $\zeta=1.5$

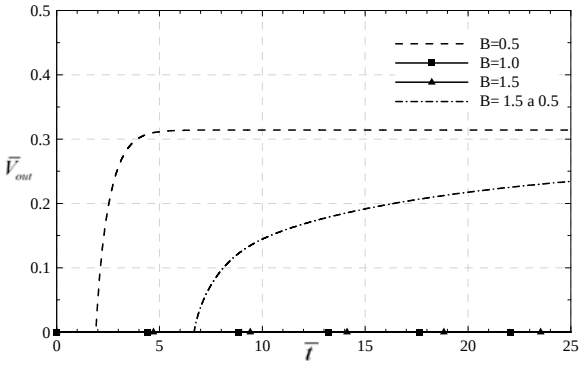

Figure 10. The effect of the Bingham number on the temporal outlet velocity variation. $Re=100.0$, $\alpha^*=0.01$, $g^*=0.1$, $\delta=0.0001$ and $\zeta=1.5$

Figure 9 depicts the inlet velocity change with time. Initially, the velocity is very high in comparison to the steady-state value for all Bingham numbers, which reflects the abrupt change of pressure at the pipe inlet. For $B=0.5$, the inlet velocity approaches a constant value approximately at $\overline{t}=4$. Note that its steady-state value is smaller than one ($\overline{V}_{in,SS}=0.311$) because the reference value is the steady-state velocity of a incompressible Newtonian fluid. The higher the Bingham numbers, the smaller the steady-state velocity, as the viscous effect is larger for Bingham flows in comparison to Newtonian flows. For $B=1.0$ and $B=1.5$, the flow initializes close to the inlet but stops soon after that; the inlet velocity drops to zero faster for the higher Bingham number. For thixotropic fluids, the Bingham number is larger than 1.0 and the inlet velocity tends to zero soon after the start-up. As the Bingham number becomes smaller than 1.0, the inlet velocity increases tending to its steady-state value ($\overline{V}_{in,SS}=0.31$).

The outlet velocity is shown in Fig. 10 for the same Bingham numbers of Fig. 9. The outlet velocity does change its initial value (zero) for $B=1.0$ and $B=1.5$, as the inlet pressure is not high enough to displace the gelified fluid portion placed at the outlet. For $B=0.5$ and the thixotropic fluid, the flow starts at the outlet and the steady-state outlet velocity is slightly higher than its inlet counterpart ($\overline{V}_{out,SS}=0.314$), as the fluid is low compressible. One can see a higher delay in the outlet flow start-up for a thixotropic fluid. The fluid will start to move at the outlet when $B<1.0$, leading to its steady-state value for $B=0.5$. A similar behavior is noted for the pressure change close the pipe outlet, as shown in Fig. 11.

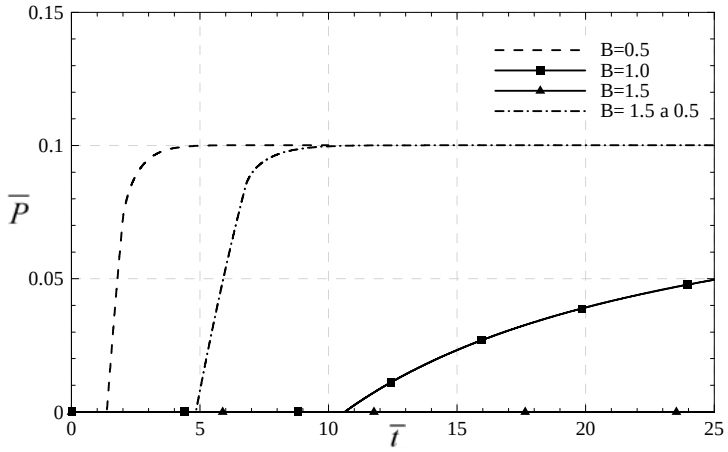

Figure 11. The effect of the Bingham number on the temporal pressure change at $\overline{z}=0.9$. $Re=100.0$, $\alpha^*=0.01$, $g^*=0.1$, $\delta=0.0001$ and $\zeta=1.5$

Figure 12 shows the pressure and velocity fields along the pipe for several instants and two Bingham numbers: $B=0.5$ and $B=1.5$. In both cases the pressure is dissipated and wave reflections do not occur. At the beginning, both pressure and velocity gradients are high, reducing with time, as the pressure wave propagates. For $B=0.5$, the pressure

wave reaches the pipe outlet and the steady-state velocity field achieves a non-zero value. On the other hand, the pressure wave does not reach the pipe outlet for $\mathrm{B} = 1.5$. The length in which the steady-state pressure gradient is not zero is proportional to the Bingham number, according to $\bar{z} = 1/\mathrm{B} = 0.67$. Note that the boldface line intercepts the $\bar{z}$ axis at 0.67 in Fig. 12b. The steady-state velocity field for the $\mathrm{B} = 1.5$ case (Fig. 12d) is zero, stressing the flow cannot be established.

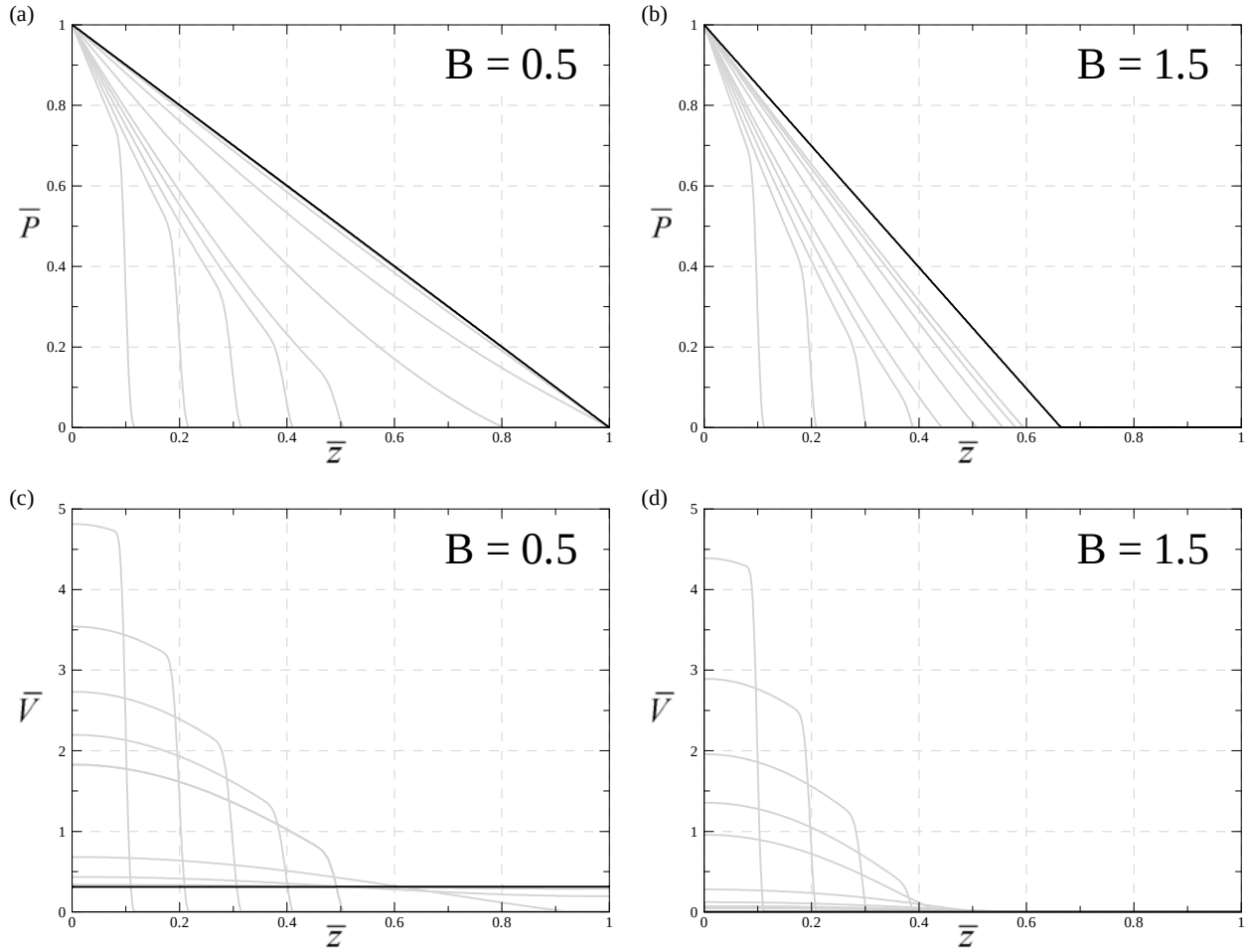

Figure 12. Spatial pressure and velocity changes for different times. $B = 0.5$ (a and c) and for $B = 1.5$ (b and d). In all Figures, the boldface line corresponds to the steady-state. The other lines are, respectively, for $\bar{t} = 0.1$, 0.2, 0.3, 0.4, 0.5, 1.0, 2.0, 3.0 and 4.0. $\mathrm{Re} = 100.0$, $\alpha^* = 0.01$, $g^* = 0.1$, $\delta = 0.0001$ and $\zeta = 1.5$

5. CONCLUSION

This work presents a 1D mathematical model for the start-up of thixotropic fluid flow in a circular or annular pipe. The governing equations of mass and momentum, together with a state and a constitutive equations, are discretized in space and time by employing the finite volume method. The upwind scheme is used as an interpolation approach and the resulting non-linear algebraic equations are solved iteratively at each time-step.

When the current model results for a non-Newtonian Bingham flow was compared with the literature ones, they showed good agreement. Besides, the governing equations were normalized and some dimensionless numbers were defined such as, the Reynolds and Bingham numbers and a dimensionless compressibility, gravity and aspect ratio. A model sensitivity analysis to the dimensionless parameters was conducted and the following was observed:

i) The smaller the Reynolds number, the higher the pressure wave dissipation and consequently, more slowly the steady-state is reached. The reason for that is the increase of the viscous in comparison to the inertia effect.

ii) For high compressible flows, the higher the aspect ratio $\delta = D_h / L$, the faster the flow response. On the other hand, for low compressible flows, the pressure oscillates along the pipe before the steady-state is reached. Besides, the higher the aspect ratio, the higher the pressure peaks magnitude, because the pipe is not long enough for pressure dissipation.

iii) As the Bingham number increases, the steady-state velocity is reduced in comparison to its Newtonian flow counterpart. However, for $\mathrm{B} \geq 1.0$, the flow starts close the pipe inlet but is unable to reach the pipe outlet. At the

steady-state, the velocity drops to zero and the fluid becomes compressed close to the pipe inlet. For a thixotropic fluid, in which the Bingham number changes from 1.5 to 0.5, the inlet pipe velocity increases considerably at the start-up and falls to zero soon after that. As the Bingham number is reduced below one, the velocity increases, leading to a non-zero steady-state value.

iv) Low compressible flows are very oscillating. As the compressibility rises, the pressure oscillation lessens or even disappears.

v) Higher pressure dissipation is observed in horizontal than in vertical flows. Besides, for low compressible cases, the pressure peaks are delayed in vertical in comparison to horizontal flows.

6. ACKNOWLEDGEMENTS

The authors would like to thanks PETROBRAS S/A, the ANP (Brazilian National Oil Agency) and the National Council for Scientific and Technological Development (CNPq) for their financial support to this work.

7. REFERENCES

Anderson, J.D., 1990, “Modern Compressible Flow: With Historical Perspective”, Ed. McGraw-Hill, N. York, United States, 650 p.

Cawkwell, M.G. and Charles, M.E., 1987, “An Improved Model for Start-up of Pipelines Containing Gelled Crude Oil”, J. of Pipelines, Vol. 7., pp. 41-52.

Chang, C., Rønningsen, H.P. and Nguyen, Q.D., 1999, “Isothermal Start-up of Pipeline Transporting Waxy Crude Oil”, J. of Non-Newtonian Fluid Mechanic, Vol. 87, Parkville, Australia, pp. 127-154.

Davidson, M.R., Nguyen, Q.D., Chang, C. and Ronningsten, H.P., 2004, “A Model for Restart of a Pipeline with Compressible Gelled Waxy Crude Oil”, J. of Non-Newtonian Fluid Mechanics, Vol. 123, No. 2-3, pp. 269-280.

Ferziger, J.H. and Peric, M., 1996, “Computational Methods for Fluid Dynamics”, Ed. Springer-Verlag, Berlin, German, 364 p.

Fontenot, J.E. and Clark, R.K., 1974, “An Improved Method for Calculating Swab and Surge Pressures and Circulating Pressures in a Drilling Well”, Soc. of Petroleum Eng. J. (SPE 4521), Vol. 14, No 5, pp 451-462.

Fortuna, A. O, 2000, “Técnicas Computacionais para Dinâmica dos Fluidos. Conceitos Básicos e Aplicações”,Ed. da Universidade de São Paulo, S. Paulo, Brazil, 426 p.

Patankar, S.V., 1980, “Numerical Heat Transfer and Fluid Flow”, Ed. Taylor & Francis, Washington, U. States, 197 p.

Sestak, J., Cawkwell, M.G., Charles, M.E. and Houskas, M.,1987, “Start-up of Gelled Crude Oil Pipelines”, J. of Pipelines, Vol. 6, Amsterdam, Holland, pp. 15-24.

Vinay, G., Wachs, A. and Agassant, J.F., 2006, “Numerical Simulation of Weakly Compressible Bingham Flows: The Restart of Pipeline Flows of Waxy Crude Oils”, J. of Non-Newtonian F. Mechics., Vol. 136, No. 2-3, Cedex, France, pp. 93-105.

Vinay, G., Wachs, A. and Frigaard, I., 2007, “Start-up Transients and Efficient Computation of Isothermal Waxy Crude Oil Flows”, J. of Non-Newtonian Fluid Mechanics, Vol. 143, No 2-3, Cedex, France, pp. 141-156.

Wachs, A., Vinay, G., and Frigaard, I., 2008, “A 1.5D Numerical Model for the Start Up of Weakly Compressible Flow of a Viscoplastic and Thixotropic Fluid in Pipelines”, J. of Non-Newtonian F. Mech., doi: 10.1016/j.jnnfm.2009.02.002.

8. RESPONSIBILITY NOTICE

The authors are the only responsible for the printed material included in this paper.